Delay and Crosstalk Aware Analysis for High Speed On-Chip Global RLC VLSI Interconnects

Apoorva Gupta, Vikas Maheshwari, Somashekhar Malipatil, and Rajib Kar

Abstract At the advanced stage of technologies, when feature size is being reduced, it is compulsory to introduce other parameters for more accurate modelling of transmission line interconnects. So mutual inductance and coupling capacitance how have become more important role for analysis of high-speed on-line VLSI interconnects. This paper introduces a mathematical aware analysis result for crosstalk noise of 'L' type RLC interconnections using mutual inductance. Two RLC interconnect lines of 'L' type, are equidistant to each other and used as 'Aggressor line' and 'Victim line' respectively, whereas, a step signal voltage is employed as input to aggressor line. Other calculative results for Delay and peak noise voltage between these two RLC electrical lines with using mutual inductance, are also introduced in this paper. This paper also shows a comparative result between our derived expression values and BKM values for simulation purpose.

Keywords Integrated circuits · RLC VLSI interconnects · Mutual inductance · Coupling capacitance · Delay · Crosstalk noise

1 Introduction

Presently, VLSI is the present level of designing and fabrication of ICs and microchips which consist of lacs of transistors on a single chip [1, 2]. In DSM region [3], now it is considered to study of inductive effect as well as capacitive-coupling effects to

A. Gupta (✉) · V. Maheshwari
Department of ECE, Guru Nanak Institutions Technical Campus, Ranga Reddy, Hyderabad, Telangana, India

S. Malipatil
Department of ECE, Malla Reddy Engineering College and Management Sciences, Medchal, Hyaderabad, Telangana, India

R. Kar
Department of ECE, National Institute of Technology, Durgapur, West-Bengal, India

V. Nath and J. K. Mandal (eds.), *Proceeding of Fifth International Conference on Microelectronics, Computing and Communication Systems*, Lecture Notes in Electrical Engineering 748,
https://doi.org/10.1007/978-981-16-0275-7_66

develop and explain the more accurate and real behaviour of on-chip VLSI interconnects. Delay and Crosstalk noise between VLSI high speed interconnected networks can have occurred due to self and mutual inductance. There are so many approaches presented [4–18] for the modelling of interconnect structures. This paper introduces use of closed loop of 'L' type RLC interconnect network. Two RLC parallel interconnects and a mutual inductance and coupling capacitance are occurred automatically. These two RLC networks are named as 'aggressor line' and 'victim line' respectively. The proposed work is much improved work of the BKM [19] model. This paper establishes a mathematical equation of crosstalk voltage of mutually inductively coupled interconnections of RLC type. This paper also introduces expressions for delay and peak noise voltage between adjacent RLC network. This paper is organized remaining follows: Sect. 2 describes Proposed models and of crosstalk voltage and delay analysis. Detailed results of simulation are discussed in portion 3 and portion 4 conclude the paper.

2 Proposed Model

Mathematical and analytical expressions for the crosstalk voltage, delay and peak crosstalk voltage are derived in the case only when victim lines are grounded and excitation is connected to aggressor line. Figure 1 shows lumped RLC model of 'L' shaped interconnection system considering Mutual Inductance coupling between the parallel lines. Step input voltage is used for the analysis of the interconnection system.

A step input voltage supply is given to the input of aggressor line which is equidistant to the victim lines. Coupling capacitance is generated because those two RLC networks are proximate to each other and mutual inductance is induced due to using inductor coil.in this paper we use 90 nm technology.

As per Moore's law, in the process of designing the ICs, the number of transistors will continue to double in every 18 months [1]. That means the same silicon area would accommodate a greater number of transistors. Transistors size is gradually getting reduced for achieving this or we can say that transistor size is shifting from one technology node to smaller technology node by using scaling process. A specific technology gets used by the industries for the period of time till the time when

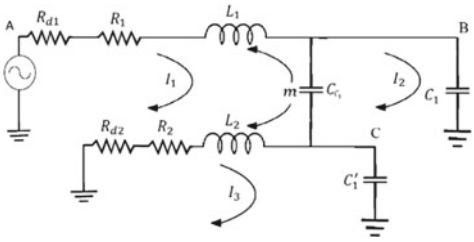

Fig. 1 Equivalent Circuit of RLC interconnects using 'L' shaped interconnect model with effect of Mutual Inductance m

the next feasible smaller technology node would be ready for implantation. For example, 180 nm technology was used mostly in 1999–2000-time period whereas 90 nm technology was used in 2004–2005. The technology's numbers represent the minimum feature size of transistor or CMOS. Minimum channel length that can be used in fabrication of CMOS or transistor is known as Feature size of transistor. These numbers are decided by dividing the previous number (technology) by square root of two ($\sqrt{2}$).

In the circuit shown in Fig. 1, at node C, we develop the mathematical expression for the voltage for RLC victim line.

On employing KVL in 1st loop:

$$V_{S1} = I_1 R_{d1} + I_1 R_1 + L_1 \frac{dI_1}{dt} - m\frac{dI_3}{dt} + \frac{1}{C_2}\int (I_1 - I_2)dt \tag{1}$$

On taking Laplace,

$$V_{S1}(s) = I_1(s)R_{d1} + I_1(s)R_1 + L_1 S I_1(s) - mSI_3(s) + \frac{1}{sC_1}[I_1(s) - I_2(s)] \tag{2}$$

$$V_{S1}(s) = \frac{(M_1 SC_1)I_1(s) - I_2(s)}{SC_1} - mSI_3(s) \tag{3}$$

Where,

$$M_1 = R_{d1} + R_1 + L_1 S \tag{4}$$

Similarly, on applying KVL in 2nd mesh,

$$\frac{1}{sC_1}[I_1(s) - I_2(s)] = \frac{1}{SC_{C1}}I_2(s) + \frac{1}{SC_1^{'}}[I_2(s) + I_3(s)]$$

$$\frac{1}{sC_1}I_1(s) - \left[\frac{1}{sC_1} + \frac{1}{SC_1^{'}} + \frac{1}{SC_{C1}}\right]I_2(s) - \frac{1}{SC_1^{'}}I_3(s) = 0 \tag{5}$$

Similarly, on applying KVL in 3rd mesh,

$$0 = I_3(s)R_{d2} + I_3(s)R_1^{'} + SL_1^{'}I_3(s) - SmI_1(s) + \frac{1}{SC_1^{'}}[I_2(s) + I_3(s)]$$

$$I_1(s)\left[-s^2 mC_1^{'}\right] + I_2(s) + \left(SM_2C_1^{'} + 1\right) = 0 \tag{6}$$

Where

$$M_2 = R_{d1} + R_1^{'} + sL_1^{'}$$

From Eqs. (3), (5) and (6), we get a matrix:

$$\begin{bmatrix} \frac{M_1SC_1+1}{SC_1} & -\frac{1}{sC_1} & -ms \\ \frac{1}{sC_1} & -\left[\frac{1}{sC_1}+\frac{1}{SC_1'}+\frac{1}{SC_{C1}}\right] & -\frac{1}{sC_1} \\ -s^2mC_1' & 1 & (SM_2C_1'+1) \end{bmatrix} \begin{bmatrix} I_1(s) \\ I_2(s) \\ I_3(s) \end{bmatrix} = \begin{bmatrix} V_{s1}(s) \\ 0 \\ 0 \end{bmatrix}$$

Let,

$$M_1SC_1 + 1 = A,\ B = -\left[\frac{1}{sC_1} + \frac{1}{SC_1'} + \frac{1}{SC_{C1}}\right],$$
$$\left(SM_2C_1' + 1\right) = C$$

Then required matrix is,

$$\begin{bmatrix} \frac{A}{sC_1} & \frac{-1}{sC_1} & -mS \\ \frac{1}{sC_1} & -B & \frac{-1}{sC_1} \\ -s^2mC_1' & 1 & C \end{bmatrix} \begin{bmatrix} I_1(s) \\ I_2(s) \\ I_3(s) \end{bmatrix} = \begin{bmatrix} V_{s1}(s) \\ 0 \\ 0 \end{bmatrix}$$

After solving by Cramer's rule [20],

$$I_1(s) = \frac{sC_1^2\left[1 - CC_1's\right]V_{s1}}{-sABCC_1C_1' - 2s^2mC_1C_1' + Bs^5m^2C_1^2C_1'^2 + AC_1 + CC_1} \tag{7}$$

$$I_2(s) = \frac{sC_1C_1'\left[ms^2C_1 - C\right]V_{s1}}{-sABCC_1C_1' - 2s^2mC_1C_1' + Bs^5m^2C_1^2C_1'^2 + AC_1 + CC_1} \tag{8}$$

$$I_3(s) = \frac{sC_1C_1'\left[1 - 3s^3mC_1C_1'\right]V_{s1}}{-sABCC_1C_1' - 2s^2mC_1C_1' + Bs^5m^2C_1^2C_1'^2 + AC_1 + CC_1} \tag{9}$$

Now, at node 'C':

$$V_c = \frac{1}{sC_1'}[I_2(s) + I_3(s)] \tag{10}$$

So,

$$V_c = \frac{sC_1C_1'V_{s1}}{sC_1'}\left[\frac{ms^2C_1 - C + 1 - Bs^3mC_1C_1'}{-sABCC_1C_1' - 2s^2mC_1C_1' + Bs^5m^2C_1^2C_1'^2 + AC_1 + CC_1}\right]$$

$$V_c = \frac{C_1V_{s1}\left[ms^2C_1 - C + 1 - Bs^3mC_1C_1'\right]}{P} \tag{11}$$

Where,

$P = -sABCC_1C_1^{'} - 2s^2mC_1C_1^{'} + Bs^5m^2C_1^2C_1^{'2} + AC_1 + CC_1$ After substituting the values of A, B and C:

$$\mathrm{P} = -\mathrm{sC_1C_1^{'}(M_1sC_1+1)}\left(\frac{\propto}{\mathrm{sC_1C_1^{'}C_{C1}}}\right)\left(\mathrm{sM_2C_1^{'}+1}\right) - 2\mathrm{s^2mC_1C_1^{'}} + \left(\frac{\propto}{\mathrm{sC_1C_1^{'}C_{C1}}}\right)\mathrm{s^5m^2C_1^2C_1^{'2}} + \mathrm{(M_1sC_1+1)C_1} + \left(\mathrm{sM_2C_1^{'}+1}\right)\mathrm{C_1^{'}}$$

Where,

$$B = \frac{\propto}{sC_{C1}C_1C_1^{'}}$$

Where,

$$\propto = C_1^{'}C_{C1} + C_{C1}C_1 + C_1C_1^{'}$$

Now,

$$\mathrm{P} = -\propto (M_1sC_1+1)\left(sM_2C_1^{'}+1\right) - 2s^2mC_1C_1^{'} + \frac{\propto}{C_1^{'}}s^4m^2C_1C_1^{'} + (M_1sC_1+1)C_1 + \left(sM_2C_1^{'}+1\right)C_1^{'}$$

After neglecting all high-power terms:

$$P = s^2C_1C_1^{'}[\propto M_1M_2 + 2m] + s\left[-\propto M_1C_1 - \propto M_1C_1^{'} + M_1C_1 + M_2C_1^{'}\right] + C_1 + C_1^{'} - \propto \tag{12}$$

Now after substituting the value of $V_{s1} = \frac{1}{s}$ (for step input voltage) & P in Eq. (11),

$$V_c = \frac{C_1\left(smC_1 - M_2C_1^{'}\right)}{s^2C_1C_1^{'}[\propto M_1M_2 + 2m] + s\left[-\propto M_1C_1 - \propto M_1C_1^{'} + M_1C_1 + M_2C_1^{'}\right] + C_1^{'} + C_1^{'} - \propto}$$

Now, let us assume:

$$X = C_1C_1^{'}[\propto M_1M_2 + 2m]$$

$$Y = -\propto M_1C_1 - \propto M_1C_1^{'} + M_1C_1 + M_2C_1^{'}$$

$$Z = C_1^{'} + C_1^{'} - \propto$$

$$P = -X^2 s + Ys + Z \tag{13}$$

$$V_c = \frac{C_1\left(smC_1 - M_2C_1^{'}\right)}{-Xs^2 + Ys + Z}$$

$$V_c = \frac{-mC_1^2 s}{Xs^2 - Ys - Z} + \frac{M_2C_1^{'}}{Xs^2 - Ys - Z}$$

$$V_c = \frac{-mC_1^2 s/X}{s^2 - \frac{Y}{X}s - \frac{Z}{X}} + \frac{M_2C_1^{'}/X}{s^2 - \frac{Y}{X}s - \frac{Z}{X}}$$

$$V_c = \frac{-mC_1^2 s/X}{\left[s - \frac{Y}{2X}\right]^2 + \left[\sqrt{\frac{-Z}{X} - \frac{Y^2}{4X^2}}\right]^2} + \frac{M_2C_1^{'}/X}{\left[s - \frac{Y}{2X}\right]^2 + \left[\sqrt{\frac{-Z}{X} - \frac{Y^2}{4X^2}}\right]^2}$$

If, $R = \left[\sqrt{\frac{-Z}{X} - \frac{Y^2}{4X^2}}\right]^2$

After taking Inverse Laplace transform:

$$V_c(t) = -\left[e^{\frac{Y}{2X}t}\cos Rt\right]\frac{mC_1^2}{X} + \left[e^{\frac{Y}{2X}t}\sin Rt\right]\frac{M_2C_1^{'}}{X}$$

$$V_c(t) = \frac{e^{\frac{Y}{2X}t}}{X}\left[M_2C_1^{'}\sin Rt - mC_1^2\cos Rt\right] \tag{14}$$

Peak time value t_{p_c} is calculated by equating first derivative of $V_c(t)$ to zero,

$$\frac{dV_c(t)}{dt} = 0$$

$$M_2C_1^{'}\frac{d}{dt}\left[e^{\frac{Y}{2X}t}\sin Rt\right] - mC_1^2\frac{d}{dt}\left[e^{\frac{Y}{2X}t}\cos Rt\right] = 0$$

After simplification we get

$$t_{p_c} = t = \frac{1}{R}\tan^{-1}\left[\frac{-RM_2C_1^{'} + \left(\frac{mC_1^2}{2}\right)\left(\frac{Y}{X}\right)}{RmC_1^2 + \left(\frac{M_2C_1^{'}}{2}\right)\left(\frac{Y}{X}\right)}\right] \tag{15}$$

Let's put the value t = t_{p_c} in Eq. (14) so that,

$$V_c(t) = \frac{t_{c(t)max}}{t_{=t_{pc}}}$$

$$V_c(t)_{max} = e^{\frac{Y}{2X}t_{p_c}}\left[M_2C_1^{'}\sin Rt_{p_c} - mC_1^2\cos Rt_{p_c}\right] \tag{16}$$

Now calculate the value of V_B:

$$V_B = \frac{1}{sC_1}[I_1(s) - I_2(s)]$$

$$V_B = \frac{V_{s1}}{sC_1}\left[\frac{sC_1^2\left[1 - BCC_1^{'}s\right] - sC_1C_1^{'}\left[ms^2C_1 - C\right]}{-sABCC_1C_1^{'} - 2s^2mC_1C_1^{'} + Bs^5m^2C_1^2C_1^{'2} + AC_1 + CC_1}\right]$$

For unit step input, $V_{s1} = \frac{1}{s}$:

$$V_B = \frac{\frac{1}{s}\left[C_1 - \frac{s\propto C_1C_1^{'}}{sC_1C_1^{'}C_{C1}}\left(1 + sM_2C_1^{'}\right) - mC_1C_1^{'}s^2 - C_1^{'}\left(1 + sM_2C_1^{'}\right)\right]}{P}$$

$$V_B = \frac{\frac{1}{s}\left[C_1 - \frac{\propto}{C_{C1}} - \frac{sM_2C_1^{'}}{C_{C1}} - mC_1C_1^{'}s^2 - M_2s\right]}{P}$$

Now let's put the value of P from expression (12) and have,

$$V_B = \frac{C_1C_{C1} - \propto -s\left(M_2C_1^{'} + M_2C_1^{'2}C_{C1}\right) - mC_1C_1^{'}C_{C1}s^2 - C_1^{'}C_{C1}}{C_{C1}s\left[-s^2C_1C_1^{'}(\propto M_1M_2 + 2m) + s\left(- \propto M_1C_1 - \propto M_2C_1^{'} + M_1C_1 + M_2C_1^{'}\right) + \left(C_1 + C_1^{'} - \propto\right)\right]}$$

$$V_B = \frac{C_1C_{C1} - \propto -C_1^{'}C_{C1}}{sPC_{C1}} - \frac{msC_1C_1^{'}C_{C1}}{PC_{C1}} - \frac{\left(M_2C_1^{'} + M_2C_1^{'2}C_{C1}\right)}{PC_{C1}}$$

$$V_B = \frac{C_1C_{C1} - \propto -C_1^{'}C_{C1}/C_{C1}}{sP} - \frac{mC_1C_1^{'}s}{P} - \frac{\left(M_2C_1^{'} + M_2C_1^{'}C_{C1}\right)/C_{C1}}{P}$$

$$V_B = V_{B1} - V_{B2} - V_{B3} \tag{17}$$

Where,

$$V_{B1} = \frac{C_1C_{C1} - \propto -C_1^{'}C_{C1}/C_{C1}}{sP}$$

$$V_{B2} = \frac{msC_1C_1^{'}}{P}$$

$$V_{B3} = \frac{\left(M_2C_1^{'} + M_2C_1^{'}C_{C1}\right)/C_{C1}}{P}$$

Putting the result of P in the equation of V_{B1} from Eq. (13)

$$V_{B1} = \frac{C_1 C_{C1} - \propto - C_1^{'} C_{C1} / C_{C1}}{s\left(-Xs^2 + Ys + Z\right)}$$

after simplification, we get,

$$V_{B1} = \frac{C_1 C_{C1} - \propto - C_1^{'} C_{C1}}{C_{C1}} \left[\frac{1}{Zs} - \frac{1}{Z\left(s + \frac{Z}{Y}\right)} \right]$$

In similar way, the expressions of V_{B2} and V_{B3} after substituting the expression of P from Eq. (13),

$$V_{B2} = \frac{\frac{-mC_1C_1^{'}}{X} s}{\left[s - \frac{Y}{2X}\right]^2 + R^2}, \quad V_{B3} = \frac{\left(M_2 C_1^{'} + M_2 C_1^{'2} C_{C1}\right) / XC_{C1}}{\left[s - \frac{Y}{2X}\right]^2 + R^2}$$

Where,

$$R = \left[\sqrt{\frac{-Z}{X} - \frac{Y^2}{4X^2}} \right]^2$$

substituting the values of V_{B1}, V_{B2}, V_{B3} in Eq. (17)

$$V_B(s) = \frac{C_1 C_{C1} - \propto - C_1^{'} C_{C1}}{C_{C1}} \left[\frac{1}{Z} \left(\frac{1}{s} - \frac{1}{\left(s + \frac{Z}{Y}\right)} \right) \right] + \frac{\frac{mC_1C_1^{'}}{X} s}{\left[s - \frac{Y}{2X}\right]^2 + R^2} + \frac{\left(M_2 C_1^{'} + M_2 C_1^{'2} C_{C1}\right) / XC_{C1}}{\left[s - \frac{Y}{2X}\right]^2 + R^2}$$

After using inverse Laplace Transform in the above expression

$$V_B(t) = \frac{\left(C_1 C_{C1} - \propto - C_1^{'} C_{C1}\right)}{C_{C1} Z} \left(1 - e^{-\left(Z / Y\right) t} \right) + \left[e^{\frac{Y}{2X} t} \cos Rt \right] \frac{mC_1 C_1^{'}}{X} + \left[e^{\frac{Y}{2X} t} \sin Rt \right] \frac{\left(M_2 C_1^{'} + M_2 C_1^{'2} C_{C1}\right)}{C_{C1} X} \tag{18}$$

On differentiating with respect to t

$$\frac{dV_B(t)}{dt} = \frac{\left(C_1 C_{C1} - \propto - C_1^{'} C_{C1}\right)}{C_{C1} Y} e^{-\left(Z / Y\right) t} + \frac{mC_1 C_1^{'}}{X} \left[\frac{Y}{2X} e^{\frac{Y}{2X} t} \cos Rt + (-R \sin Rt) e^{\frac{Y}{2X} t} \right] + \frac{\left(M_2 C_1^{'} + M_2 C_1^{'2} C_{C1}\right)}{C_{C1} X} \left[\frac{Y}{2X} e^{\frac{Y}{2X} t} \sin Rt + R \cos Rt e^{\frac{Y}{2X} t} \right]$$

Peak time value is calculated by equating first derivative to zero,

$$\frac{\left(C_1C_{C1}-\propto-C_1^{'}C_{C1}\right)}{C_{C1}Y}e^{-\left(Z/Y\right)t_p}+\cos Rt_pe^{\frac{Y}{2X}t_p}\left[\frac{Y}{2X^2}mC_1C_1^{'}+\frac{R\left(M_2C_1^{'}+M_2C_1^{'2}C_{C1}\right)}{C_{C1}X}\right]+$$
$$\sin Rt_pe^{\frac{Y}{2X}t_p}\left[\frac{Y}{2X^2C_{C1}}\left(M_2C_1^{'}+M_2C_1^{'2}C_{C1}\right)-\frac{R}{X}mC_1C_1^{'}\right]=0$$

Let us assume for simplicity,

$$q=\frac{\left(C_1C_{C1}-\propto-C_1^{'}C_{C1}\right)}{C_{C1}Y}$$

$$u=\frac{Y}{2X^2}mC_1C_1^{'}+\frac{R\left(M_2C_1^{'}+M_2C_1^{'2}C_{C1}\right)}{C_{C1}X}$$

$$v=\frac{Y}{2X^2C_{C1}}\left(M_2C_1^{'}+M_2C_1^{'2}C_{C1}\right)-\frac{R}{X}mC_1C_1^{'}$$

After simplification above equation becomes,

$$q.e^{-\left(Z/Y\right)t_p}+\cos Rt_pe^{\frac{Y}{2X}t_p}.u+\sin Rt_pe^{\frac{Y}{2X}t_p}.v=0$$

$$q.e^{-\left(Z/Y\right)t_p}+e^{\frac{Y}{2X}t_p}\left(u.\cos Rt_p+v.\sin Rt_p\right)=0 \tag{19}$$

After simplification and approximation to lower degree terms of above Eq. (19), we get

$$t_p=\frac{2XY(u+q)}{qZ-2XYvR-uY^2} \tag{20}$$

$$t_p=\frac{H}{I}$$

where,

$$H=2XY(u+q),\ I=qZ-2XYvR-uY^2$$

After substituting the values of t_p in equation, so now

$$V_{Bmax}(t)=\left(\frac{C_1C_{C1}-\propto-C'_1C_{C1}}{C_{C1}Z}\right)\left(1-e^{\left(Z/Y\right)\left(H/I\right)}\right)$$
$$+\frac{mC'_1C_{C1}}{X}\left[e^{\left(\frac{Y}{2X}\right)\left(\frac{H}{I}\right)}\cdot\cos\left(\frac{RH}{I}\right)\right]+\frac{M_2C'_1+M_2C'^2_1C_{C1}}{C_{C1}X}\left[e^{\left(\frac{Y}{2X}\right)\left(\frac{H}{I}\right)}\cdot\sin\left(\frac{RH}{I}\right)\right] \tag{21}$$

The expressions for peak delay time and peak voltages at node C and B are discussed by Eqs. (15), (16), (20) and (21) respectively. The essential proposed

crosstalk voltage and peak crosstalk noise voltage respectively at node C are discussed by Eqs. (14) and (16).

3 Simulation Result and Discussion

Figure-1 shows simulation set-up of two L type High speed RLC mutually coupled interconnection system having 1000 μm of length. High performance CPU system designs typically consist of such type of bus structures. Symmetrical Step signal having finite and equal rise/fall time of 10 ps is used to excite the aggressor line. It is assumed that the interconnection system is identical and symmetrically distributed by considering that the system is connected with identical size of inverters for drivers and loads. Variations in the input slew times values up to 200 ps are used for the simulation of Mutually coupled interconnection system connected with identical driver size.

For the testing and verification purpose, we have compared our proposed model values with BKM [19] model values to show the novelty of our proposed work. This comparison was done on the same set of circuit parameters. Our work is much-improved version of BKM model [19] for the same L-interconnect model with the consideration of mutual inductance for high operating frequencies. Comparison of simulated results at node C for the expression given by Eq. (16) for proposed model and BKM model are demonstrated in Table 1 for various input slew times. Table 2 discusses the comparison of aggressor line voltage described by Eq. (21) with BKM model values and our proposed model for the various input slew values. Comparative results for the peak times t_{pc} and t_{pb} at node C and node B of the victim line and aggressor line described by Eqs. (15) and (20) respectively is discussed in Table 3 and Table 4. Comparative results for proposed model Aggressor voltage, BKM and SPICE for different values of T_s are shown in Figs. 2, 3 and 4 respectively. Similarly, comparative results for aggressor line voltage, victim line peak time and aggressor line peak time values from proposed model and the values from SPICE simulations are shown in Figs. 5, 6, 7, 8, 9, 10, 11, 12 and 13 respectively.

.

Table 1 Comparative analysis for peak crosstalk noise received from proposed model and BKM [19]

R_{D1} (Ω)	R_{D2} (Ω)	C_L (fF)	$T_s = 0$		$T_s = 100$		$T_s = 200$	
			BKM values (mV)	Our model values (mV)	BKM values (mV)	Our model values (mV)	BKM values (mV)	Our model values (mV)
10	10	1.2	121	101	161	147	210	181
10	15	1.2	139	118	179	167	231	197
15	20	1.2	147	143	202	189	245	231
15	25	2.4	182	167	238	216	279	268
15	50	2.4	221	192	271	243	291	294

Table 2 Comparative analysis for aggressor line voltage received from proposed model and BKM [19]

R_{D1} (Ω)	R_{D2} (Ω)	C_L (fF)	$T_s = 0$		$T_s = 100$		$T_s = 200$	
			BKM values (mV)	Our model values (mV)	BKM values (mV)	Our model values (mV)	BKM values (mV)	Our model values (mV)
10	10	1.2	0.761	0.551	0.951	0.745	1.17	1.002
10	15	1.2	0.872	0.649	1.02	0.812	1.26	1.012
15	20	1.2	1.01	0.998	1.35	0.903	1.41	1.213
15	25	2.4	1.29	1.123	1.48	1.212	1.68	1.534
15	50	2.4	1.43	1.324	1.71	2.012	1.74	2.121

Table 3 Comparative analysis for victim line peak time got from proposed model and BKM [19]

R_{D1} (Ω)	R_{D2} (Ω)	C_L (fF)	$T_s = 0$		$T_s = 100$		$T_s = 200$	
			BKM values (nS)	Our model values (nS)	BKM values (nS)	Our model values (nS)	BKM values (nS)	Our model values (nS)
10	10	1.2	23.12	17.13	37.73	23.87	59.29	32.73
10	15	1.2	27.34	18.95	48.24	26.12	77.92	37.49
15	20	1.2	39.71	20.32	73.84	28.78	98.28	39.15
15	25	2.4	45.64	21.78	91.27	30.19	103.37	41.29
15	50	2.4	59.59	22.12	103.12	32.19	118.23	44.29

Table 4 Comparative analysis for aggressor line peak time vn ‘received from proposed model and BKM [19]

R_{D1} (Ω)	R_{D2} (Ω)	C_L (fF)	$T_s = 0$		$T_s = 100$		$T_s = 200$	
			BKM values (nS)	Our model values (nS)	BKM values (nS)	Our model values (nS)	BKM values (nS)	Our model values (nS)
10	10	1.2	10.54	7.13	28.43	10.2	46.54	15.17
10	15	1.2	25.32	7.98	36.21	12.28	59.32	16.29
15	20	1.2	38.65	8.54	47.32	15.19	73.72	18.54
15	25	2.4	55.23	10.19	65.81	18.39	82.82	20.18
15	50	2.4	68.84	10.36	75.32	21.26	99.32	22.87

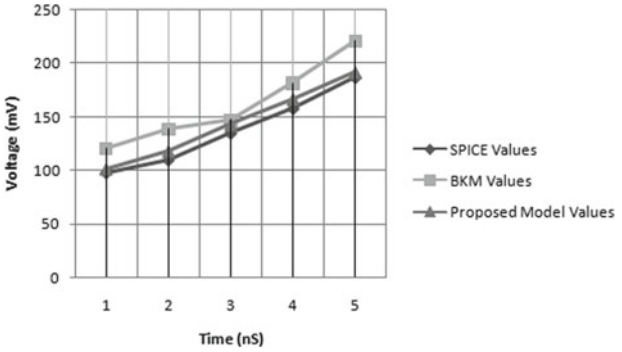

Fig. 2 Comparative graph of peak crosstalk noise obtained from proposed model, SPICE and BKM with $T_s = 0$

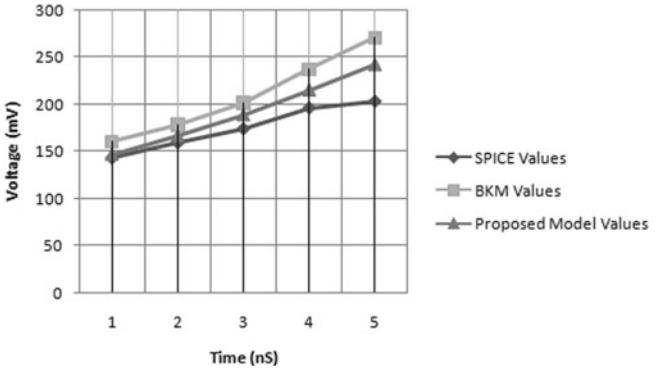

Fig. 3 Comparative graph of peak crosstalk noise obtained from proposed model, SPICE and BKM with $T_s = 100$

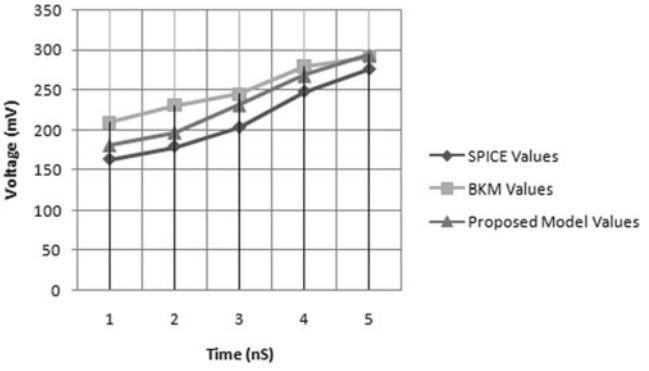

Fig. 4 Comparative graph of peak crosstalk noise obtained from proposed model, SPICE and BKM with $T_s = 200$

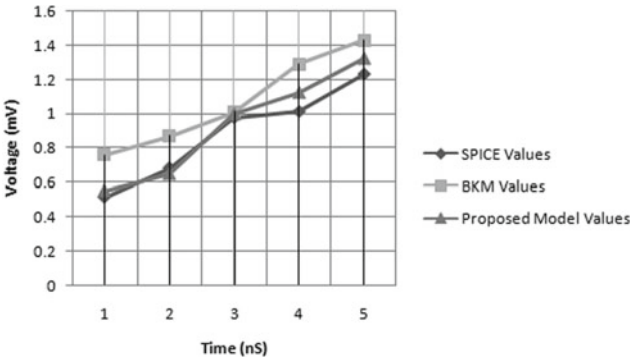

Fig. 5 Comparison of aggressor line voltage obtained from proposed model, SPICE and BKM with $T_s = 0$

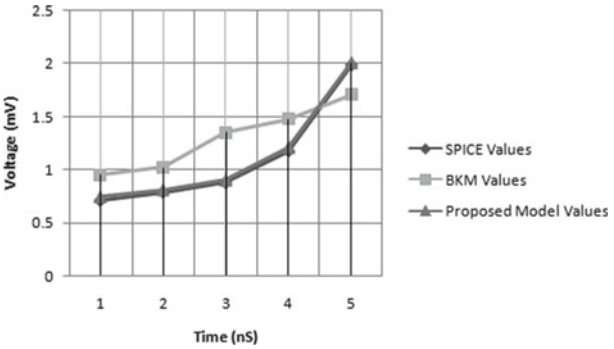

Fig. 6 Comparison of aggressor line voltage obtained from proposed model, SPICE and BKM with $T_s = 100$

Fig. 7 Comparison of aggressor line voltage obtained from proposed model, SPICE and BKM with $T_s = 200$

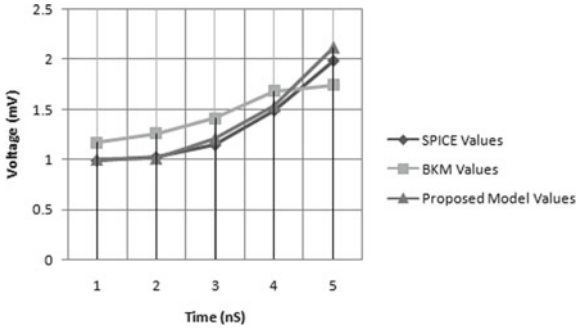

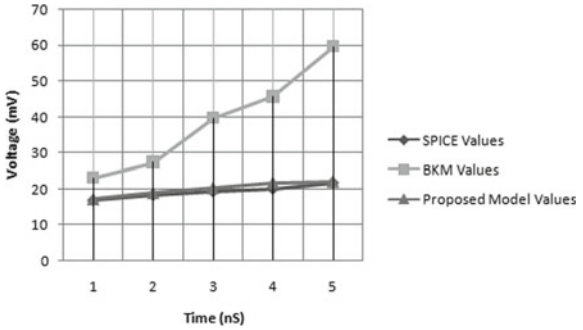

Fig. 8 Comparison victim line peak time obtained from proposed model, SPICE and BKM with $T_s = 0$

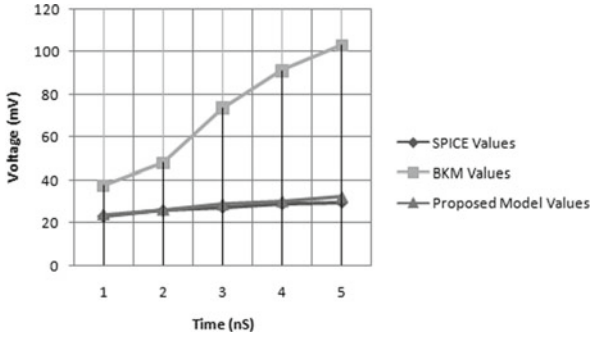

Fig. 9 Comparison victim line peak time obtained from proposed model, SPICE and BKM with $T_s = 100$

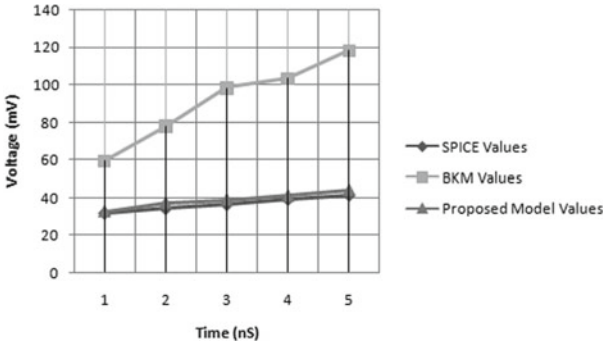

Fig. 10 Comparison victim line peak time obtained from proposed model, SPICE and BKM with $T_s = 200$

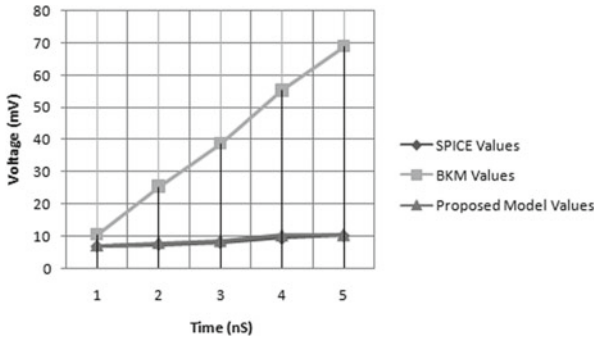

Fig. 11 Comparison of aggressor line peak time obtained from proposed model, SPICE and BKM with $T_s = 0$

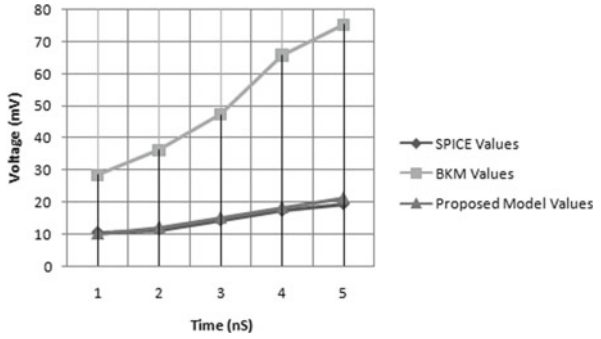

Fig. 12 Comparison of aggressor line peak time obtained from proposed model, SPICE and BKM with $T_s = 100$

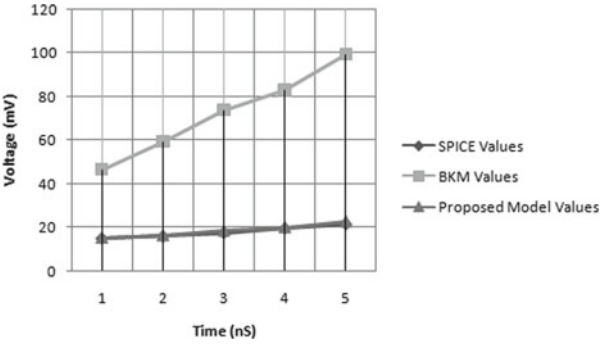

Fig. 13 Comparative graph of aggressor line peak time obtained from proposed model, SPICE and BKM with $T_s = 200$

After analysing the simulated result related Figs. 2, 3, 4, 5, 6, 7, 8, 9 and 10 and Tables 1, 2, 3 and 4, we can easily find out the novelty and importance of our proposed model in comparison to BKM [19] model. By considering mutual inductance in between two coupled interconnection models, our proposed model becomes more realistic and generic as it follows SPICE results better than BKM model. Deviation in between BKM model values with SPICE values is very large therefore; BKM model becomes appropriate in current scenario.

4 Conclusion

Proposed research work discussed about the mathematical analysis of delay and crosstalk voltage in mutually coupled RLC VLSI interconnection structures. The derived models for crosstalk voltage and delay are found precise as simulation results are very close to SPICE. The L-type RLC mutually coupled interconnection system is proposed in this research work. The correctness and validity of the research work is demonstrated by the simulation results. Simulation results shows that the proposed models are having less than 10% error comparable to the results obtained from the SPICE.

References

1. Wu B (2017) High bandwidth IC interconnects with silicon interposers and bridges for 3D multi-chip integration and packaging. In IEEE Semiconductor Technology International Conference (CSTIC) China, 12–13 April 2017, pp 1–3
2. Zhang XJ, Jiang W, Gao L, li H (2016) Impact of cross talk on signal integrity of high-speed density ceramic package for IC. In: IEEE international conference on electronic packaging technology Wuhan, 16–19 August 2016
3. Wu SY, Liew BK, Young KL, Yu CH, Sun SC (1999) Analysis of interconnect delay for 0.18 μm technology and beyond. In: IEEE International Conference on Interconnect Technology, San Francisco, CA, USA May 1999, pp 68–70
4. Agrawal Y, Chandel R (2016) Crosstalk analysis of current-mode signalling-coupled RLC interconnects using FDTD technique. IETE Tech Rev 33(2):148–159
5. Gupta A, Maheshwari V, Sharma S, Kar R (2015) Crosstalk noise and delay analysis for high speed on-chip global RLC VLSI interconnects with mutual inductance using 90 nm process technology. In: International Conference on computing on computing, communication and automation (ICCCA-2015), 15–16 May 2015, pp 1215–1219
6. Fattah G, Masoumi N (2018) Comprehensive evaluation of crosstalk and delay profiles in VLSI interconnect structure with partially coupled lines. J Iran Assoc Electric Electron Eng 14(4):41–54
7. Rebelli S, Nestala BR (2018) An efficient MRTD model for analysis of crosstalk in CMOS-driven coupled cu interconnects. Radio Eng 27(2):532–540
8. Rebelli S, Nistala BR (2020) A multiresolution time domain (MRTD) method for crosstalk noise modeling of CMOS-gate-driven coupled MWCNT interconnects. IEEE Trans Electromagn Compat 62(2):521–531

9. Bhattacharya S, Rahaman DDH (2017) Analysis of temperature- dependent crosstalk for graphene nanoribbon and copper interconnects. IETE J Res 10(20):187–205
10. Maheshwari V, Gupta S, Khare K, Yadav V, Kar R, Mandal D, Bhattacharjee AK (2012) Efficient coupled noise estimation for RLC on-chip interconnect. In: IEEE Symposium on Humanities, Science and Engineering Research (SHUSER-2012), Kuala Lumpur, Malaysia, 24–27 June 2012, pp 1125–1129
11. Hunagund PV, Kalpana AB (2010) Crosstalk noise modeling for RC and RLC interconnects in deep submicron VLSI circuits. J Comput 2:60–65
12. Kar R, Maheshwari V, Mal AK, Bhattacharjee AK (2010) Delay analysis for on-chip VLSI interconnect using gamma distribution function. Int J Comput Appl 1(3):65–68. Article 11
13. Peng X, Pan Z (2017) The analytical model for crosstalk noise of current-mode signaling in coupled RLC interconnects of VLSI circuits. J Semiconductors 38(9):095003
14. Mudavath R, Naik BR (2018) Estimation of far end crosstalk and near end crosstalk noise with mutually coupled RLC interconnect models. In: IEEE International Conference on Communication and Signal Processing India, 3–5 April 2018, pp 0198–0201
15. Maheshwari V, Suvra R, Kar D, Mandal AKB (2012) Analytical crosstalk modelling of on-chip RLC global interconnects with skin effect for ramp input. Procedia Technol 6:814–821
16. Mudavath R, Naik BR, Gugulothu B (2019) Analysis of crosstalk noise for coupled microstrip interconnect models in high-speed PCB design. In: International Conference on Electronics, Information, and Communication (ICEIC) New Zealand, 22–29 January 2019
17. Chhotray SK, Mohapatra DD, Dash SS, Swain S (2013) An analytical delay expression for deep sub-micron RLC interconnect. Int J Eng Res Appl 3(5):1727–1730
18. Chowdhury MMH (2004) Noise Analysis and Design Methodologies in Deep Sub-Micron VLSI circuits. PhD Dissertation, North-Western university
19. Kumar B, Maheshwari V, Dhubkariya DC, Kar R (2013) Analytical modeling of crosstalk noise and delay for high speed on-chip global RLC VLSI interconnects. J Electron Dev 17:1452–1456
20. Strang G (1998) Linear Algebra and its Applications, 3rd ed. Harcourt Brace Jovanich, Inc.